



Full Text View

[Volume 32, Issue 12 \(December 2002\)](#)

Journal of Physical Oceanography

Article: pp. 3396–3407 | [Abstract](#) | [PDF \(1.32M\)](#)

Temporal and Spatial Structure of the Equatorial Deep Jets in the Pacific Ocean*

Gregory C. Johnson

NOAA/Pacific Marine Environmental Laboratory, Seattle, Washington

Eric Kunze

Applied Physics Laboratory, University of Washington, Seattle, Washington

Kristene E. McTaggart and Dennis W. Moore

NOAA/Pacific Marine Environmental Laboratory, Seattle, Washington

(Manuscript received November 28, 2001, in final form May 10, 2002)

DOI: 10.1175/1520-0485(2002)032<3396:TASSOT>2.0.CO;2

ABSTRACT

The spatial and temporal structure of the equatorial deep jets (EDJs) in the Pacific Ocean is investigated using CTD station data taken on the equator from 1979 through 2001. The EDJs are revealed in profiles of vertical strain, ξ_z , estimated from the CTD data in a stretched vertical coordinate system. The majority of synoptic meridional sections were occupied over an 8-yr span west of the date line. Two-decade equatorial time series are available at both 110°W and 140°W. Analysis shows the expected equatorial trapping of ξ_z but yields little new detailed information about the EDJ meridional structure. Analysis of the equatorial data yields novel results. The EDJs are most easily seen in the eastern Pacific (at and east of 140°W). There, they may be isolated from the influence of higher-frequency Rossby waves generated by surface forcing. Spectral analysis of equatorial ξ_z profiles shows a significant and coherent peak at 400-sdbar vertical wavelength (with $N_o = 1.56 \times 10^{-3} \text{ s}^{-1}$) from 95°W to 142°W. This peak has very long zonal scales. It exhibits a very slow mean downward migration of $4.2(\pm 0.5) \times 10^{-7} \text{ sdbar s}^{-1}$ [$13(\pm 2) \text{ sdbar yr}^{-1}$]. Whether this migration is steady or intermittent is difficult to ascertain. However, over the two-decade record length, the EDJs shift downward by only about two-thirds of a vertical wavelength. Hence it is no surprise that previous

Table of Contents:

- [Introduction](#)
- [Data and processing](#)
- [Qualitative description](#)
- [Quantitative analysis](#)
- [Discussion](#)
- [REFERENCES](#)
- [FIGURES](#)

Options:

- [Create Reference](#)
- [Email this Article](#)
- [Add to MyArchive](#)
- [Search AMS Glossary](#)

Search CrossRef for:

- [Articles Citing This Article](#)

Search Google Scholar for:

- [Gregory C. Johnson](#)
- [Eric Kunze](#)

observational analyses of the EDJs in the Pacific, limited to 16 months or less, had difficulty finding any significant vertical migration.

- [Kristene E. McTaggart](#)
- [Dennis W. Moore](#)

1. Introduction

The equatorial deep jets (EDJs) are equatorially trapped zonal currents of a few to several hundred meter vertical wavelength that exist through much of the water column in all the oceans and persist for decades. An early report of the EDJs was made using acoustic dropsonde measurements taken in 1976 in the Indian Ocean ([Luyten and Swallow 1976](#)).


In short order, dropsonde and CTD measurements were taken in various locations across the equatorial Pacific Ocean. Observations at 168°E and 179°E revealed equatorially trapped motions and isopycnal displacements with vertical wavelengths of a few hundred meters and timescales greater than the month-long cruise on which the data were collected ([Eriksen 1981](#)). Zonal coherences were short, perhaps because the measurements straddled the Gilbert Islands. The EDJs were observed in zonal velocity profiles near the equator and 110°W ([Hayes and Milburn 1980](#)). They were observed with a transect of zonal velocity profiles along the equator between 159°W and 125°W ([Leetmaa and Spain 1981](#)), with zonal coherence over at least 1000 km. The Pacific Equatorial Ocean Dynamics (PEQUOD) program included a 16-month time series of short meridional sections of velocity along 159°W that showed EDJs that were remarkably steady in time, perhaps migrating upward by 50 m over the duration of the record ([Firing 1987](#)). A set of zonal velocity profiles between 153° and 138°W in the equatorial central Pacific, repeated on three cruises in January 1981, February 1982, and April 1982 ([Ponte and Luyten 1989](#)) showed distinct spectral peaks near 350 and 560 stretched meters (the former being the EDJs). Given the sampling, zonal length scales and vertical migration rates were difficult to determine.

In the Indian Ocean, temporally sparse data (three cruises over 4 years) have been recently analyzed to show that the EDJs there have a longer vertical wavelength than in the Pacific, and to suggest that observed phases are consistent with an annual current reversal ([Dengler and Quadfasel 2002](#)). Analysis of sparse Atlantic data (three cruises over 3 years) shows that EDJs there also have a longer vertical wavelength than in the Pacific, that they have a long zonal scale, and again suggests that EDJ observed phases are consistent with an annual current reversal ([Gouriou et al. 1999](#)). However, data from a 20-month current meter mooring are analyzed to suggest that Atlantic EDJs are quasi steady for intervals of a year or more, punctuated by intermittent phase and amplitude variability ([Send et al. 2002](#)). This result is reminiscent of analysis of the best temporally resolved EDJ dataset in the central Pacific ([Firing 1987](#)). Both studies caution that inferring periodicity from sparse data is risky.

A number of dynamical interpretations have been advanced for the EDJs. Early efforts attempted to explain the EDJs in the context of linear equatorial wave theory. The quadrature in phase between isopycnal displacement and zonal velocity has been used to advance the hypothesis that they are mainly manifestations of Kelvin waves ([Eriksen 1981, 1982](#)). However, an attempt to interpret the EDJ signature in the central Pacific in terms of linear equatorial wave theory was ambiguous ([Ponte and Luyten 1989](#)). Furthermore, significant potential vorticity anomalies in the EDJs are inconsistent with equatorial Kelvin waves, but broadly resemble first meridional mode Rossby waves, though, given the low frequencies involved, this interpretation is difficult to justify ([Muench et al. 1994](#)). The EDJs have also been modeled as linear superpositions of Rossby and Kelvin waves, with a complex structure dependent on the basin geometry, the mean stratification, and the forcing characteristics ([McCreary 1984](#)). Recent alternatives to the linear equatorial wave interpretations are the hypotheses that EDJs derive their energy from equatorial inertial instability ([Hua et al. 1997](#)) or by the deposition of internal wave momentum at critical layers ([Muench and Kunze 1999, 2000](#)).

At any rate, the EDJs are in geostrophic balance ([Eriksen 1982; Muench et al. 1994](#)). If they follow Kelvin wave dynamics, stretching of the density field on the equator corresponds to eastward velocity anomalies, analogous to the Equatorial Undercurrent, and equatorial density squashing to westward anomalies. For first-meridional-mode Rossby wave dynamics, the velocity anomalies reverse sign. This means that historical CTD data can be exploited to analyze the long zonal and temporal scales of these motions. Since there are many more deep CTD stations than deep velocity profiles in the Pacific, analysis of the former is potentially valuable. The variable analyzed below to diagnose stretching and squashing of isopycnals is vertical strain, ξ_z . The vertical coordinate used is Wentzel–Kramers–Brillouin–Jeffreys (WKBJ)-scaled stretched pressure (sdbar). The CTD data available in the equatorial Pacific are described, and their processing detailed in [section 2](#). A qualitative look at the structure of the EDJs is given in [section 3](#). Spectral and harmonic analysis of the EDJs allows more quantitative estimates of the EDJ characteristics in [section 4](#). The results are discussed in [section 5](#).

2. Data and processing

Since 1979, 3132 CTD stations reaching at least 1100 dbar have been occupied within $\pm 8.5^\circ$ of the equator in the Pacific, with 1529 of these reaching at least 2996 dbar ([Fig. 1](#) ). These data originate from a wide variety of programs. They have

been taken by PMEL investigators during maintenance of the TAO array, compiled from NODC, and obtained from other sources.

The temporal, zonal, meridional, and vertical coverage of these data is highly heterogeneous (Fig. 1). There are 32 synoptic cross-equatorial meridional sections with deep station spacing of 1° latitude or closer. The nine meridional World Ocean Circulation Experiment sections crossing the equatorial Pacific are distributed along it at roughly equal distances. Nonetheless, 27 of the 32 sections are found west of the date line, with 18 at 142°E and 165°E (cf. Gouriou and Toole 1993). The remainder of the off-equatorial stations are distributed across the Pacific, but concentrated at Tropical Atmosphere–Ocean Array (TAO) mooring locations: ±2°, ±5°, and ±8°. The most data are found along the equator, but only a few longitudes boast deep stations occupied at quasi-annual or shorter intervals for more than a decade: 110°W (22 yr), 140°W (21 yr), 165°E (15 yr), and 170°W (13 yr).

For all 3132 CTD stations reaching at least 1100 dbar, temperature and salinity are linearly interpolated onto a 1-dbar pressure grid. These records are then smoothed by convolution with a 19-point (10-dbar halfwidth) Hanning filter and subsampled at 10-dbar intervals. At this point, buoyancy frequency squared, N^2 , is estimated for each point by centered differences over 20-dbar spans. The buoyancy frequency, N , is estimated by taking the square root of the absolute value of $N^2 = -(g/\rho)(\partial\rho/\partial z)$, then multiplying by the sign of N^2 to preserve apparent inversions. Here, g is the acceleration of gravity, z is the vertical axis (depth), and ρ is the potential density referenced to a local central pressure.

Waves propagating vertically through the ocean exhibit apparently changing wavelengths and amplitudes as the background stratification changes with depth. WKBJ scaling and stretching (Leaman and Sanford 1975) compensates for the effects of varying stratification in the vertical by stretching the vertical coordinate system and scaling the signal amplitudes. After WKBJ scaling and stretching, variations of wavelength and amplitude owing to vertical variations in stratification are minimized, allowing identification of waves using standard spectral methods.

Mean profiles of N and N^2 for the entire tropical Pacific are required for WKBJ stretching and scaling, respectively. Here $\langle N \rangle$ (Fig. 2a) and $\langle N^2 \rangle$ denote these quantities, which are the result of a two-step process. First, profiles of N and N^2 from all stations are averaged at each pressure regardless of time or location. Then these quantities are further smoothed with a 49-point (250-dbar halfwidth) Hanning filter. The filter is also weighted by the number of stations contributing to the mean profiles at each pressure.

WKBJ scaling is applied using the $\langle N \rangle$ profile to obtain stretched pressure from pressure, with a reference $N_o = 1.56 \times 10^{-3} \text{ s}^{-1}$ chosen to be the vertical mean of $\langle N \rangle$, so the 0–6200-dbar (sdbar) ranges of the stretched and unstretched pressures are identical (Fig. 2b). Stretched and unstretched pressures have equivalent vertical scales near 1733 dbar (4481 sdbar), where $\langle N \rangle = N_o$ (Fig. 2a). There is significant variation in N and N^2 within the surface thermocline and in the abyss across the tropical Pacific. However, the analysis presented here focuses on the water column between 660 and 2996 dbar (2970 and 5370 sdbar), where these quantities do not vary as much horizontally.

Previous studies have used vertical displacement, $\zeta = (\rho - \langle \rho \rangle)/(\partial \langle \rho \rangle / \partial z)$, from the CTD data to look at the EDJ signature in the density field. If the EDJs are in geostrophic balance, then ζ and zonal velocity should be in quadrature on the equator (Eriksen 1981). The quantity ζ can be WKBJ-scaled by multiplication with $(\langle N \rangle / N_o)^{1/2}$. However, ζ is strongly aliased by station-to-station bias errors in salinity (Eriksen 1981). Such small errors in salinity can lead to large offsets in ζ , as ρ for a biased station deviates erroneously and systematically from $\langle \rho \rangle$, especially in regions of small vertical stratification. Thus, to use ζ when combining datasets from a large number of sources with varying qualities of salinity calibration would introduce noise which could significantly impact the analysis. Rather than trying to harmonize various data sets through ad hoc adjustments of salinity on a station-by-station basis, we chose to study another variable. This variable involves a vertical derivative of the density field, so effects of systematic salinity offsets among stations are eliminated.

Vertical strain, $\xi_z = (N^2 - \langle N^2 \rangle) / (\langle N^2 \rangle)$, is closely related to N^2 and reveals stretching and squashing of the density field. For Kelvin wave dynamics, equatorial negative anomalies of N^2 (stretching) are associated with positive (eastward) zonal velocity, and squashing with westward velocity. Thus, ξ_z is a prewhitened, normalized representation of stretching and squashing anomalies and should be directly out of phase with zonal velocity on the equator. The raw ξ_z profiles are estimated from the original 10-dbar centered difference N^2 profiles and $\langle N^2 \rangle$. These raw ξ_z profiles are transformed from their original uniform 10-dbar pressure grid to a uniform 10-sdbar stretched pressure grid in two ways (Fig. 3). For the quantitative analysis (interpolated ξ_z), the raw values are linearly interpolated where $\langle N \rangle$ exceeds N_o . Where N_o exceeds $\langle N \rangle$,

so simple linear interpolation would alias short wavelength information, the raw values are smoothed minimally through use of a loess filter ([Cleveland and Devlin 1988](#)) with a half-power point at 10 sdbar to preserve the energy for wavelengths of 20 sdbar and longer. For qualitative description (vertically smoothed ξ_z) the raw values are gridded over the entire stretched pressure range using a loess filter with a half power point at 200 sdbar. The reason for this choice of vertical smoothing is apparent in [section 4](#).

3. Qualitative description

The meridional, temporal, and zonal characteristics of the EDJs are illustrated using the 200-sdbar vertically smoothed ξ_z profiles in a few synoptic meridional sections and equatorial time series sections at a few longitudes. After some exploration, the portion of the water column where the EDJs were most apparent was found to be 2970–5370 sdbar (660–2996 dbar). The analysis in [section 4](#) will show that the EDJ signature in ξ_z is located near a vertical wavelength of 400 sdbar, in agreement with previous results discussed in [section 1](#). Since ξ_z is prewhitened, vertically smoothed ξ_z profiles ([Fig. 3](#)) allow a visual focus on this vertical wavelength, by removing much of the shorter wavelength energy. These vertically smoothed ξ_z profiles are used in this section only, for illustrative purposes.

Equatorial trapping of energy at these longer wavelengths is apparent in typical meridional–vertical sections in the western (165°E) and eastern (110°W) Pacific ([Fig. 4](#)). At both longitudes, most of the energy is contained within $\pm 1.5^\circ$ of the equator. If one were interpreting these features as linear equatorial waves, one would expect Kelvin waves to have maxima of ξ_z on the equator and be more equatorially trapped than first-meridional-mode Rossby waves, which would exhibit off-equatorial maxima within roughly a degree of the equator. Examples of both such characteristics can be seen in these and the other 30 synoptic meridional sections. Unfortunately, most of these synoptic meridional sections are located in the western Pacific, whereas zonally and temporally coherent EDJ signatures are most obvious in the eastern Pacific. As an aside, the large-amplitude off-equatorial features at 110°W at and below 5200 sdbar (2650 dbar) are signatures of the general circulation: low-latitude plumes extending far to the west from the East Pacific Rise ([Johnson and Talley 1997](#)).

Temporal–vertical sections using ξ_z profiles within $\pm 0.5^\circ$ of the equator at well-sampled longitudes show clear and coherent EDJ signatures, especially at 110°W, but also at 140°W ([Fig. 5](#)). Apparent vertical discontinuities in the contours are caused by the combination of high-frequency noise and the inclusion of stations that were occupied very close in time. Contouring these nearby stations without any temporal smoothing gives a visual indication of the noise levels in even these vertically smoothed ξ_z profiles. Some of the sources of noise at the EDJ wavelength are internal gravity waves including internal tides, high (e.g., annual period and shorter) frequency Kelvin waves, and high-frequency Rossby waves. Even with this noise, a vertical wavelength near 400 sdbar is apparent and the EDJs appear to slowly migrate downward, especially at 110°W. The mean migration rate is very slow, although given the noise ascertaining the character of this migration is difficult. EDJ vertical phase propagation may be steady or intermittent. At any rate, over the two decades spanned by the data, the EDJs shift downward by less than a vertical wavelength. In addition, although the EDJ signal is less coherent at 140°W, phasing of the EDJs appears similar to that at 110°W, suggesting very long zonal scales.

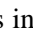

In the central and western Pacific, at 170°W and 165°E ([Fig. 6](#)), the time series of ξ_z are shorter and sparser. The 400-sdbar vertical wavelength signal in the deeper halves of these sections appears to migrate slowly downward as it does in the east. However, the upper halves of the western time series are not so simple. The 170°W section shows a strong transient feature in the upper half of the stretched pressure range displayed near the time of the 1997–98 El Niño. These features suggest the possibility of surface forcing from interannual variability even at these depths. The 165°E section, which is better sampled temporally than the one at 170°W, appears to favor shorter vertical wavelengths and perhaps some relatively rapid upward phase propagation in the upper half of the displayed range, although it is not well resolved.


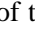
In summary, meridional ξ_z sections reveal that energy at the EDJ wavelength is equatorially trapped across the Pacific. A qualitative examination of ξ_z time series at four well-sampled longitudes across the Pacific suggests that the EDJ signature is stronger and more coherent in the eastern Pacific than in the west. At middepth in the east, the EDJs are apparent as a 400-sdbar vertical wavelength signal that migrates downward very slowly, although not necessarily steadily, over the record length. These patterns are more obvious at 110°W than at 140°W. In the central and western Pacific, this same pattern may be present in the lower half of the sections. However, the situation is more complex in the upper part of these sections. It is possible that EDJs in the upper parts of the central and western Pacific sections are better masked by phenomena such as higher-frequency Rossby waves excited by surface forcing as they propagate westward and downward ([Kessler and McCreary 1993](#)).

4. Quantitative analysis

Here, we use spectral and harmonic methods for a quantitative analysis of the ξ_z field and the EDJs. We quantify the meridional structure of the ξ_z field as a function of latitude and vertical wavelength in the western and eastern Pacific. A 400-sdbar vertical wavelength peak, the EDJ signature, stands out on the equator in the eastern Pacific. This peak is coherent over more than two decades temporally and more than 5000 km zonally, with a slow mean downward phase migration and no significant zonal structure. The peak is sufficiently coherent that it is possible to fit a time–depth plane wave to it and determine the vertical wavelength and vertical phase propagation that minimize variance in the data.





The following analysis uses a subset of the 1541 CTD stations that reach to at least 2996 dbar and focuses on the middle portion of the water column, 2970–5370 sdbar (660–2996 dbar). This 2400-sdbar span is in the portion of the water column where $\langle N \rangle$ has minimal horizontal variations, and is a convenient interval for a Fourier decomposition that resolves the EDJ wavelength. Instead of the vertically smoothed ξ_z profiles discussed qualitatively in [section 3](#), the interpolated ξ_z profiles, which resolve energy down to 20-sdbar wavelengths, are used in all the analysis that follows. Since ξ_z is a normalized, prewhitened quantity, little preparation is necessary. For the time–depth plane wave fitting, the interpolated ξ_z profiles are analyzed as is. Prior to the Fourier decomposition, a 10% cosine taper is applied to each profile. No zero-padding is used, so the vertical wavelengths resolved by the profile segments covering 2400 sdbar at 10-sdbar intervals range from 20 to 2400 sdbar.

Equatorial trapping of ξ_z energy is obvious in both the western ([Fig. 7a](#) : 132.5°–167.5°E) and eastern ([Fig. 7b](#) : 142.5°–92.5°W) Pacific. To explore this trapping, the composite spectra over large longitude bins are estimated by averaging all spectra within $\pm 0.5^\circ$ latitude of the equator, as well as within $\pm 0.5^\circ$ latitude of the following distances from the equator: $\pm 1^\circ$, $\pm 2^\circ$, $\pm 5^\circ$, and $\pm 8^\circ$ latitude, which are the best-sampled locations. The $\pm 8^\circ$ spectra are not shown because they are not significantly different from the $\pm 5^\circ$ spectra. In the western Pacific, energy levels decay monotonically with increasing distance from the equator (as far as $\pm 5^\circ$ latitude) over vertical wavelengths from 40 to 400 sdbar. There is no obvious narrowband peak anywhere in the spectra that might be associated with the EDJs, and no significant coherence is found across this longitude and time range at any of the distances from the equator. EDJs may be present but not evident because of more energetic broadband processes. In the eastern Pacific, the meridional trapping is even more pronounced. Over a wide band of vertical wavelengths, energy levels roughly halve with each increasing distance from the equator analyzed out to $\pm 5^\circ$ latitude. In the eastern Pacific, spectra on and $\pm 1^\circ$ from the equator both show a distinct peak around 400 sdbar, the signature of the EDJs.

A closer look at the ξ_z spectrum on the equator in the eastern Pacific reveals the coherent signature of the EDJs. Over this longitude and time range, only the peak on the equator at 400-sdbar vertical wavelength stands outside two standard errors of the mean estimated from the individual spectra of the 170 profiles (95% confidence limits: [Fig. 8a](#) ). In addition, this wavelength is coherent at far above the 95% confidence limits ([Fig. 8b](#) ), where each unique pair of the 170 profiles used is assumed independent from the others.

The longitude range over which the EDJ signature is most distinct and coherent, 142.5°–92.5°W in the eastern Pacific, was chosen after much exploration. Expanding the range to the west or east degraded the EDJ signal. Spectral analysis of the equatorial ξ_z data in 15° longitude bins (not shown) shows a 400-sdbar spectral peak at 95°W, 110°W, 125°W, and 140°W, but not farther west. This peak is most energetic at 95°W, but with only 17 profiles in that bin, its coherence of 0.14 is well below the 95% confidence limit of 0.21. At 110°W, with 59 profiles, the peak stands out as significant, and its coherence of 0.36 (by far the highest in any longitude bin) greatly exceeds the 95% confidence limit of 0.06. At 125°W and 140°W the peaks are also significant with coherences well above the 95% confidence limits, but neither EDJ signature in these longitude bins is as strong as that at 110°W.

The pressure range used here was similarly picked by exploration. As mentioned above, the EDJs appear to be coherent over some deeper portion of the water column to the west. However, in the west, the EDJs do not appear to persist over enough of the water column to allow spectral analysis that would resolve the 400-sdbar vertical wavelength.

The vertical migration of the EDJs can be quantified using vertical phase information at 400-sdbar vertical wavelength from the equatorial eastern Pacific profiles. Vertical phase lags for all the profile pairs are associated with both time ([Fig. 9a](#) ) and longitude ([Fig. 9b](#) ) lags. Coherence magnitude is significant over nearly all temporal ([Fig. 9c](#) ) and zonal ([Fig. 9d](#) ) lags when the data are sorted into 20 equal-sized subsets by either temporal or zonal lags, so the propagation information also can be extracted by fitting the phase lags to a single time–longitude plane (constrained to pass through the origin) against time and longitude lags. The fit is done by iteration, starting by assuming time–longitude stationarity, and adjusting the phase lags to lie within $\pm 180^\circ$ of each new time–longitude plane estimate until a stable solution is found.

Uncertainties given are twice the error of the planar fit (Fig. 9): conservatively assuming that each profile, rather than each unique profile pair, gives a degree of freedom) that correspond to 95% confidence limits. The average phases of the 20 lag-sorted subsets cluster around the planar fit phase estimates. The mean downward phase migration speed is $4.2(\pm 0.5) \times 10^{-7}$ sdbar s^{-1} [$13(\pm 2)$ sdbar yr^{-1}].

The zonal wavenumber estimated from this analysis is quite uncertain, at $1.5(\pm 1.6) \times 10^{-3}$ cycles per degree, again with 95% confidence limits (Fig. 9b). Thus the best estimate of the zonal attributes involves eastward propagation with a formal wavelength of about 670° longitude, nearly twice the circumference of the earth. This zonal scale is much longer than the analyzed longitude range of about 50° , so the large uncertainties are to be expected. Within the uncertainties, the EDJs could be zonally invariant.

To estimate better the vertical wavelength, a time–depth plane wave is fit to the equatorial eastern Pacific region. Zonal variations are ignored, since zonal scales are clearly very long and ill-determined. This fit is made using the same one-hundred and seventy 2400-sdbar interpolated segments of ξ_z used for the spectral analysis, but without applying the 10% cosine taper used for the spectral work. The vertical wavelength is $413(\pm 13)$ sdbar, agreeing with the spectral results. The downward propagation speed is $4(\pm 1) \times 10^{-7}$ sdbar s^{-1} [$13(\pm 4)$ sdbar yr^{-1}]. Error estimates are made using a delete-one jackknife (Efron 1982), where each segment is viewed as independent and errors quoted are twice the standard error, or roughly 95% uncertainties. Not surprisingly, the value for vertical propagation is very similar to that from the Fourier decomposition. While the vertical wavelength is more tightly constrained, the uncertainty in the vertical propagation is about twice as large as that from spectral methods.

While the best plane wave fit accounts for only 1.4% of the total variance, this reduction is sharply localized to the vertical wavelength and vertical phase propagation characteristic of the EDJs. The 400-sdbar vertical wavelength peak accounts for 4.7% of the total variance in the eastern equatorial Pacific spectrum (Fig. 8a). Thus, the plane wave fit accounts for nearly one-third of the variance at the EDJ vertical wavelength in this region. Some of the remaining variance in this wavelength could be due to noise sources discussed above. A simple plane-wave model does not allow for the potential of intermittent phase propagation, or any other deviations from regular behavior. If this model is inadequate to describe the EDJs, its restrictive simplicity could also help account for the relatively small fraction of the variance explained.

5. Discussion

Vertical strain, ξ_z , is analyzed across the middepth equatorial Pacific Ocean using historical CTD data extending over more than two decades. The use of ξ_z instead of vertical displacement reduces noise from salinity calibration offsets, allowing use of CTD data from many different sources without introduction of too much error.

Equatorial intensification of energy is demonstrated over a wide range of vertical wavelengths. This finding is not new (Eriksen 1981; Ponte and Luyten 1989), except that previous results were for zonal velocity and vertical displacement, not ξ_z . Since ξ_z should be directly out of phase with zonal velocity on the equator and in quadrature with vertical displacement, the results here should not be too surprising. Equatorial trapping in the eastern Pacific is more pronounced than in the western Pacific.

While ξ_z in the equatorial western Pacific exhibits only a broadband and incoherent equatorial enhancement of energy over a wide range of vertical wavelengths, a significant spectral peak at the 400-sdbar vertical wavelength is found along the equator in the eastern Pacific. This wavelength is equivalent to that of the peak that Ponte and Luyten (1989) found in zonal velocity (but not vertical displacement) at 350 sm, given the differences in N_θ between this study and theirs. The peak is coherent over more than two decades, from 1979 to 2001, and coherent over more than 5000 km zonally, between 142° and 95° W. This significant peak with long zonal and temporal coherences is a new result, obtainable because of the relatively large quantity of historical CTD data available. This significant peak and coherence, strongest at 110° W, do not persist to the west of 140° W, at least over the upper portion of the stretched pressure range analyzed. This result is consistent with historical results across the Pacific, where the EDJs were much more clearly defined, zonally, and temporally coherent in the eastern (Ponte and Luyten 1989; Leetmaa and Spain 1981) and perhaps central (Firing 1987) than in the western Pacific (Eriksen 1981). Perhaps the EDJs are clearly seen only in a deep, eastern shadow zone (where surface forcing does not directly reach), and elsewhere, higher-frequency surface energy, such as Rossby waves propagating downward as they move westward (Kessler and McCreary 1993), masks the EDJs.

This coherent and significant 400-sdbar peak of ξ_z in the equatorial eastern Pacific, the EDJ signature, exhibits mean downward phase migration of about 4×10^{-7} sdbar s^{-1} (13 sdbar yr^{-1}). This mean migration is extremely slow, on the

order of the magnitude of globally averaged abyssal upwelling rates. However, with the data at hand, it is difficult to see if this vertical migration is steady or intermittent, as suggested by other studies ([Firing 1987](#); [Send et al. 2002](#)). At any rate, observations of this vertical migration over two decades are novel. Given the slow mean speed and possible intermittency of vertical phase migration, it is no wonder that earlier observational programs with a maximum duration of 16 months could not discern it clearly.

The 400-sdbar vertical wavelength and the mean downward migration of $4.2(\pm 0.5) \times 10^{-7}$ sdbar s^{-1} can be used to estimate a period of 30(± 4) yr, a very dangerous exercise given the relative shortness of the 22-yr record length. More than another century of observation may be necessary to assess adequately any EDJ periodicity. Nonetheless, using this information with $N_o = 1.56 \times 10^{-3} s^{-1}$, one can estimate zonal wavenumbers formally consistent with a linear equatorial Kelvin wave and a first-meridional-mode equatorial Rossby wave. (These waves would be vertical mode 31 in a 6200-sdbar depth ocean.) The theoretical zonal wavenumber for a first-meridional-mode equatorial Rossby wave (-3.5×10^{-3} cycles per degree) does not fall within the observational estimates of $1.5(\pm 1.6) \times 10^{-3}$ cycles per degree. Interestingly, the theoretical Kelvin wave zonal wavenumber (1.2×10^{-3} cycles per degree) is quite consistent with the best estimate from the observations.

However, there are a number of significant impediments to interpreting the EDJs as remotely forced linear equatorial waves. First, the physical meaning of zonal wavelengths ranging from a few times the length of the basin to a few times the circumference of the earth is unclear. Nevertheless, the zonal phase information from this analysis is formally consistent with a Kelvin wave, but not a first-meridional-mode Rossby wave. If one were to interpret the EDJs as a remotely forced linear equatorial Kelvin wave, the downward phase propagation would imply upward energy propagation, hence bottom generation or reflection. However, propagation times from the bottom seem prohibitively long given short vertical scales and the presence of dissipation ([Muench and Kunze 1999, 2000](#)), and it is difficult to imagine the origin of such low-frequency forcing from below or above. Also, previous work on the EDJ meridional structure suggests that it is consistent with a first meridional mode Rossby wave, but not a Kelvin wave ([Muench et al. 1994](#)). The zonal phase speeds for the Kelvin wave ($0.1 m s^{-1}$) and the first-meridional-mode Rossby wave ($0.03 m s^{-1}$) are about the same size as the observed zonal velocities of the EDJs ([Eriksen 1981](#); [Firing 1987](#); [Ponte and Luyten 1989](#)), suggesting the potential importance of advection, and perhaps nonlinearity. With this combination of results, remotely forced linear equatorial waves seem poor models for the data.

All of the above points to the likelihood of alternative hypotheses such as equatorial inertial instability generating the jets and setting their vertical scale ([Hua et al. 1997](#)), perhaps subsequently fed and maintained by internal-wave momentum deposition at critical layers ([Muench and Kunze 1999, 2000](#)). Such mechanisms for local generation and maintenance of short vertical wavelength features at middepth eliminate the difficulties inherent in remotely forcing the EDJs. However, locally forced EDJs could still roughly conform to equatorial wave dynamics.

In summary, this study has confirmed previous results that EDJs are more easily seen in the eastern than western Pacific. In the equatorial eastern Pacific, a significant and coherent EDJ signature with a 400-sdbar vertical wavelength peak is found in vertical displacement, ξ_z . This signature is clearest at 110°W, but the EDJ peak is significant and coherent over the 22-yr record and a zonal range from 142° to 95°W, a distance exceeding 5000 km. The zonal phase information suggests the jets could be considered zonally invariant across the eastern Pacific. The mean downward phase migration of 13 sdbar yr^{-1} at the 400-sdbar wavelength in the eastern Pacific is remarkably slow, but may not be steady. A number of questions remain regarding dynamics, forcing, and maintenance of the EDJs. It is hoped that these observations will provoke more research directed toward answering these questions.

Acknowledgments

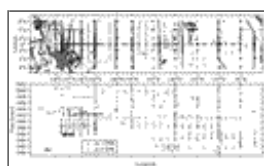
This work was funded by the NOAA Office of Oceanic and Atmospheric Research and the NOAA Office of Global Programs. The analysis presented here would not have been possible without the careful and sustained work of the officers, crew, and scientific parties of the many scientific programs involved in collecting deep CTD data in the equatorial Pacific. Conversations with Eric D'Asaro, William Kessler, LuAnne Thompson (as usual), and Mike Wallace were useful. Comments from Eric Firing and two anonymous reviewers improved the manuscript.

REFERENCES

Cleveland W. S., and S. J. Devlin, 1988: Locally weighted regression: An approach to regression analysis by local fitting. *J. Amer. Stat. Assoc.*, **83**, 596–610. [Find this article online](#)

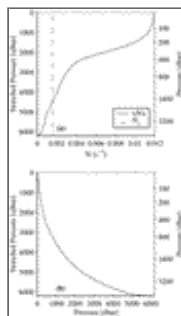
- Dengler M., and D. Quadfasel, 2002: Equatorial deep jets and abyssal mixing in the Indian Ocean. *J. Phys. Oceanogr.*, **32**, 1165–1180. [Find this article online](#)
- Efron B., 1982: *The Jackknife, the Bootstrap, and Other Resampling Plans*. CBMS-NSF Regional Conference Series in Applied Mathematics, Vol. 38, SIAM, 92 pp.
- Eriksen C. C., 1981: Deep currents and their interpretation as equatorial waves in the western Pacific Ocean. *J. Phys. Oceanogr.*, **11**, 48–70. [Find this article online](#)
- Eriksen C. C., 1982: Geostrophic equatorial deep jets. *J. Mar. Res.*, **40**, 143–157, (Suppl.),. [Find this article online](#)
- Firing E., 1987: Deep zonal currents in the central equatorial Pacific. *J. Mar. Res.*, **45**, 791–812. [Find this article online](#)
- Gouriou Y., and J. Toole, 1993: Mean circulation of the upper layers of the western equatorial Pacific. *J. Geophys. Res.*, **98**, 22495–22520. [Find this article online](#)
- Gouriou Y., B. Bourles, H. Mercier, and R. Chuchla, 1999: Deep jets in the equatorial Atlantic Ocean. *J. Geophys. Res.*, **104**, 21217–21226. [Find this article online](#)
- Hayes S. P., and H. B. Milburn, 1980: On the vertical structure of velocity in the eastern equatorial Pacific. *J. Phys. Oceanogr.*, **10**, 633–635. [Find this article online](#)
- Hua B. L., D. W. Moore, and S. Le Gentil, 1997: Inertial non-linear equilibration of equatorial flows. *J. Fluid Mech.*, **331**, 345–371. [Find this article online](#)
- Johnson G. C., and L. D. Talley, 1997: Deep tracer and dynamical plumes in the tropical Pacific Ocean. *J. Geophys. Res.*, **102**, 24953–24964. [Find this article online](#)
- Kessler W. S., and J. P. McCreary, 1993: The annual wind-driven Rossby wave in the subthermocline equatorial Pacific. *J. Phys. Oceanogr.*, **23**, 1192–1207. [Find this article online](#)
- Leaman K. D., and T. B. Sanford, 1975: Vertical energy propagation of inertial waves: A vector spectral analysis of velocity profiles. *J. Geophys. Res.*, **80**, 1975–1978. [Find this article online](#)
- Leetmaa A., and P. F. Spain, 1981: Results from a velocity transect along the equator from 125° to 159°W. *J. Phys. Oceanogr.*, **11**, 1030–1033. [Find this article online](#)
- Luyten J. R., and J. C. Swallow, 1976: Equatorial undercurrents. *Deep-Sea Res.*, **23**, 999–1001. [Find this article online](#)
- McCreary J. P. Jr., 1984: Equatorial beams. *J. Mar. Res.*, **42**, 395–430. [Find this article online](#)
- Muench J. E., and E. Kunze, 1999: Internal wave interactions with equatorial deep jets. Part I: Momentum-flux divergences. *J. Phys. Oceanogr.*, **29**, 1453–1467. [Find this article online](#)
- Muench J. E., and E. Kunze, 2000: Internal wave interactions with equatorial deep jets. Part II: Acceleration of the jets. *J. Phys. Oceanogr.*, **30**, 2099–2110. [Find this article online](#)
- Muench J. E., E. Kunze, and E. Firing, 1994: The potential vorticity structure of equatorial deep jets. *J. Phys. Oceanogr.*, **24**, 418–428. [Find this article online](#)
- Ponte R. M., and J. Luyten, 1989: Analysis and interpretation of deep equatorial currents in the central Pacific. *J. Phys. Oceanogr.*, **19**, 1025–1038. [Find this article online](#)
- Send U., C. Eden, and F. Schott, 2002: Atlantic equatorial deep jets: Space–time structure and cross-equatorial fluxes. *J. Phys. Oceanogr.*, **32**, 891–902. [Find this article online](#)

Figures



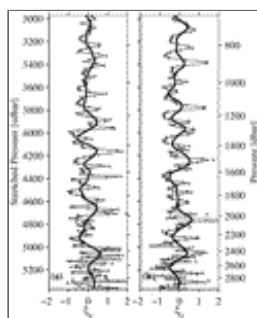
[Click on thumbnail for full-sized image.](#)

FIG. 1. (a) Latitude–longitude map of deep CTD stations taken since 1979. (b) Longitude–time map of all CTD stations within $\pm 0.5^\circ$ of the equator. Stations reaching to at least 1100 dbar but not 2996 dbar (\times) are differentiated from those extending to or beyond 2996 dbar ($+$).



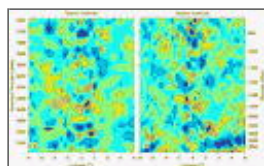
[Click on thumbnail for full-sized image.](#)

FIG. 2. (a) Profile of $\langle N \rangle$ (s^{-1}) (solid line) plotted against stretched pressure (sdbar) with reference unstretched pressures (dbar) on the right-hand side; N_o (dash-dot line) is shown for reference. (b) Unstretched pressure (dbar) plotted against stretched pressure (sdbar)



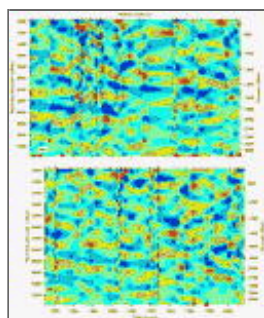
[Click on thumbnail for full-sized image.](#)

FIG. 3. Typical equatorial raw values ($+$), interpolated profiles (thin line), and vertically smoothed (200-sdbar half-power point loess filtered) profiles (thick line) of ξ_z on the equator at (a) 165°E and (b) 110°W . Data are plotted against stretched pressure (sdbar), with reference unstretched pressures (dbar) on the right-hand side



[Click on thumbnail for full-sized image.](#)

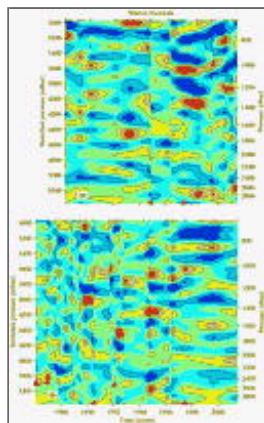
FIG. 4. Meridional–vertical sections of smoothed ξ_z at (a) 165°E and (b) 110°W . Contour interval is 0.2 for black lines and 1.0 for white lines, with negative values blue and positive values red. CTD station locations are shown on section tops. Magenta triangles [e.g., 5°S , 4950 sdbar (2300 dbar) at 165°E] indicate maximum pressures of profiles ending above or near 5370 sdbar (2996 dbar). Vertical axis is stretched pressure (sdbar) with reference unstretched pressures (dbar) on the right-hand side



[Click on thumbnail for full-sized image.](#)

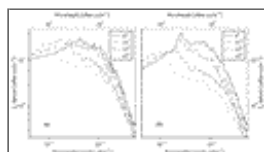
FIG. 5. Temporal–vertical sections of smoothed ξ_z within $\pm 0.5^\circ$ of the equator at (a) 110°W and (b) 140°W . Magenta triangles indicate maximum pressures of profiles ending above or near 5370 sdbar (2996 dbar). Apparent vertical discontinuities are caused

by contouring stations occupied close in time without any temporal smoothing. These artifacts are retained to indicate noise levels. Other details follow [Fig. 4](#)



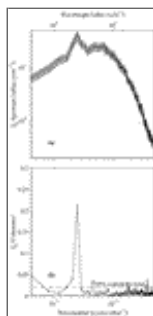
[Click on thumbnail for full-sized image.](#)

FIG. 6. Temporal–vertical sections of smoothed ξ_z within $\pm 0.5^\circ$ of the equator at (a) 170°W and (b) 165°E . Other details follow [Fig. 5](#)



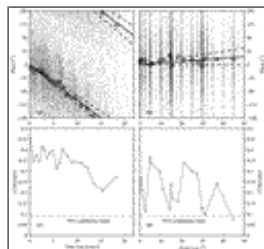
[Click on thumbnail for full-sized image.](#)

FIG. 7. Mean vertical wavelength power spectra of ξ_z using data between 2970 and 5370 sdbar (660 and 2996 dbar) from stations grouped by longitude within $\pm 0.5^\circ$ of various distances from the equator (0° : solid, $\pm 1^\circ$: dash–dot, $\pm 2^\circ$: dashed, $\pm 5^\circ$: dotted) in (a) western Pacific (132.5°E – 167.5°E) and (b) eastern Pacific (142.5°E – 92.5°W). Since ξ_z has no dimension, its power spectra have the somewhat unusual dimensions of sdbar cycle^{-1}



[Click on thumbnail for full-sized image.](#)

FIG. 8. (a) Mean vertical wavenumber power spectrum of ξ_z from the 170 profiles extending to 5370 sdbar (2996 dbar) between 142.5°E and 92.5°W within $\pm 0.5^\circ$ of the equator. Spectra are estimated using data between 2970 and 5370 sdbar (660 and 2996 dbar). Shading encompasses twice the standard error of the mean (95% confidence limits). Since ξ_z has no dimension, its power spectrum has the somewhat unusual dimensions of sdbar cycle^{-1} . (b) Magnitude of spectral coherence for these same profiles with 95% confidence limit



[Click on thumbnail for full-sized image.](#)

FIG. 9. Vertical phases and coherence magnitudes of ξ_z at 400-sdbar wavelength from Fig. 8. Individually vertical phases (small dots) and averages of 20 equal-sized lag-sorted subsets (thick circles; see text) are plotted against (a) temporal and (b) zonal lags. Phase (solid lines) from time–longitude plane iteratively fit (see text) to individual phases against lags are plotted with twice the standard error (dashed lines) for 95% confidence limits. Zonal propagation is taken into account when plotting vertical phases versus temporal lags and vice versa, using results of the final planar fit. Coherence magnitudes of these 20 equal-sized lag-sorted subsets plotted against (c) temporal and (d) zonal lags with 95% confidence limits

* Pacific Marine Environmental Laboratory Contribution Number 2441.

Corresponding author address: Dr. Gregory C. Johnson, NOAA/Pacific Marine Environmental Laboratory, 7600 Sand Point Way N.E., Bldg. 3, Seattle, WA 98115-6349. E-mail: gjohnson@pmel.noaa.gov

top ▲



© 2008 American Meteorological Society [Privacy Policy and Disclaimer](#)
Headquarters: 45 Beacon Street Boston, MA 02108-3693
DC Office: 1120 G Street, NW, Suite 800 Washington DC, 20005-3826
amsinfo@ametsoc.org Phone: 617-227-2425 Fax: 617-742-8718
[Allen Press, Inc.](#) assists in the online publication of *AMS* journals.